IIETA International Information and Engineering Technology Association
Advancing the World of Information and Engineering

Journal of New Materials for Electrochemical Systems
Vol.23, No.2, April, 2020, pp. 123-132
http://new-mat.org
http://iieta.org/journals/jnmes

Interfacial Microstructure Analysis of AA2024 Welded Joints by Friction Stir Welding

T Rajkumar[1], K Raja[2], K Lingadurai[3], S D Vetrivel[4] and A. Godwin Antony[5]

[1, 5] Department of Mechanical Engineering, K. Ramakrishnan College of Technology, Trichy 621 112, Tamil Nadu, India
[2, 3] Department of Mechanical Engineering, University College of Engineering, Dindigul 624622, Tamil Nadu, India
[4] Department of Robotics and Automation Engineering, PSG College of Technology, Coimbatore-641004, Tamil Nadu, India

Corresponding Author Email: vpantrajkumar@gmail.com

ABSTRACT

Process of joining different components by the application of external heat has resulted in induced stress on metals. Friction stir welding has been developed in order to avoid such residual stress development while joining. In this present work, aluminium alloy AA2024 plates were welded by using Friction stir welding process. The experiments were conducted for different combinations of parameters such as rotational speed, transverse speed and axial load. Welded joints developed were tested for mechanical and microstructure analysis. Mechanical joints developed have a maximum hardness of 147.6 hv in nugget zone and maximum tensile strength of 368.76 N/mm^2. Response surface analysis carried out has revealed that transverse speed and rotational speed has high impact on the hardness and tensile strength respectively. The grains at the nugget zone were very fine and uni-axed improving their tensile strength.

Keywords: *friction stir welding, AA2024 aluminium alloy, Response surface method, mechanical properties, microstructural characteristics*

Received: March-26-2020, Accepted: April-29-2020, https://doi.org/10.14447/jnmes.v23i2.a09

1. INTRODUCTION

The weight reduction in the aircraft structures is a current issue that aeronautic industries are facing, due to that new alloy are introduced to meet the needs of the industries. Al-Cu, alloy has been used as an aerospace material for many years primarily due to its high weldability and high specific strength in addition to the excellent cryogenic properties so to be successfully used for manufacturing of cryogenic fuel tanks for space launchers. When welding with al-Cu alloys by fusion welding gives more defects like porosity, hot cracking and liquation cracking thus alternative welding method should be chosen [1-5]. Friction stir welding (FSW) is an innovative, environment friendly and energy-efficient process which has evolved as favorable joining process for welding aluminum alloys. It eliminates the welding defects caused by melting and solidification in conventional welding techniques. So many research works have been carried out in this field to understand the effect of various process parameters like rotational speed, traverse speed, welding time, axial load and tool pin geometry. Attempts were made to attain an optimized condition through various techniques such as Taguchi's method, Response Surface Method, Neural Network, Fuzzy logic and other evolutionary algorithms. The material AA2024 has a typical microstructure and crystallographic characteristics that alloy it to be suitable for aerospace applications involving higher strength, structural rigidity, good joining ability, etc., [6-8]. Chanakyan et al. [9] investigated the effects of process parameters on ultimate tensile strength and micro hardness using RSM. Parameters like rotational speed, traverse speed and axial load were considered for developing mathematical models for predicting UTS and HV. Li et al. [10] developed 7A04-T6 aluminum joints through FSW process. Fine grains were observed at nugget zone with mis-orientation of grain boundary. The dynamic recrystallization resulted in great reduction of micro cracks propagation. Refining of grain microstructure and improvement in mechanical property were achieved by laser local heat treatment (LLHT).

Mehta et al. [11] investigated Al-Mg joints formed via FSW method through various mechanical and microstructural test evaluations. Al_3Mg_2 & $Al_{12}Mg_{17}$ intermetallic compounds were visualized throughout the testing at nugget zone. Cooling assisted has improved strength through intermetallic compound reduction in the weld. About 73% increment in joining efficiency of process was observed with the assistance of cooling. Choi et al. [12] evaluated the fracture strength and tried optimizing the same for pure Ti and Al metal joints formed through FSW. The large amount of interfacial sedimentation of Ti particle on Al metal and vice versa was observed at high probe offset and rotational speed, despite the base metal thickness. Superior tensile strength of Ti/Al joint was achieved via suppression of Ti fragments formation during material flow in FSW. Reduced offsetting of probe and optimized rotation of tool resulted in increased strength along with proper intermetallic layer formation at nugget zone. Shen et al. [13] studied about the influence of tool profile over the formation of voids in Al6022-T4/Al7075-T6 weld joints developed through refill spot FSW. The present work aims at understanding the influence of FSW process of AA2024 alloy over the mechanical properties and microstructural analysis. FSW process parameters will be optimized using response surface methodology to achieve better metallurgical and mechanical properties of the similar joint.

2. EXPERIMENTAL SETUP

The experimentation was carried out on a friction stir welding step up with special arrangement for work holding and tool holding as shown in Figure 2. The workpiece material

chosen for this work was aluminium alloy AA2024 plates of thickness 3 mm and rectangular cross section of 99.8 mm X 49.8 mm. The alloy material was chosen based on its application in aerospace industries. It holds special characteristics like fracture toughness, higher tensile strength and resistance towards corrosion [1]. The chemical composition of AA2024 and D2 tool steel as tool material are provided in Table 1 and 2. The critical process parameters as dependant variables chosen for the current study were rotational speed, traverse speed and axial load. The experiment was performed with three factors such as rotational speed, traverse speed and axial load with five levels and mathematical models are developed using the response surface methodology (RSM), and the adequacy was checked using ANOVA. The model developed using RSM-central composite design was analysed using interaction surface plots. The ultimate tensile strength and hardness are taken as response variables for analysing the effect of process variables. The total experimental design followed for machining was provided in Table 3. Design expert software was used to predict the regression equation with 20 trials central composite design for the present study. The value of tilt angle and penetration depth were fixed as 1^0 degree and 2.7 mm respectively during the operation [15]. FSW process was conducted using D2 tool steel with 2.7 mm pin length and 15 mm shoulder diameter. The pin is fabricated with straight cylindrical profile and 3 mm pin root diameter. Samples prepared from welded specimen were etched with Keller's reagent (190 ml H_2O, 5 ml HNO_3, 3 ml HCl and 2 ml HF) for approximately 120 s.

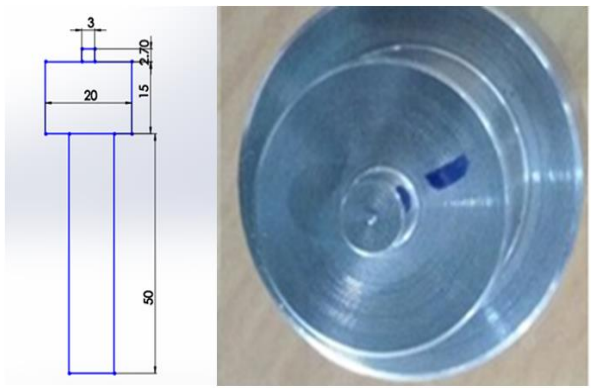

Figure 1. Tool Profile (Cylindrical Tool)

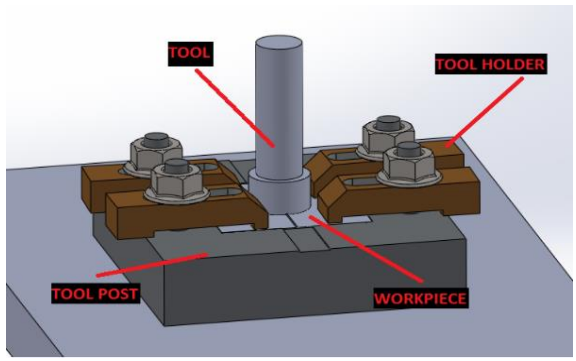

Figure 2. Schematic layout of experimental setup

Table 1. Chemical composition of D2 Tool steel

Element	C	Mn	Si	Co	Cr	Mo	V	Ni	Cu	Fe
wt. %	1.4-1.6	0.6	0.6	1	11-13	0.7-1.2	1.1	0.3	0.25	balance

3. RESULTS AND DISCUSSION

Experimentation was carried out following central composite design approach of response surface methodology. The total 20 trial runs were listed in Table 3. The layout of the experimental setup is shown in Figure 3. Mechanical properties of hardness and tensile strength of the welded specimen were measured suiting to the application [1]. The results revealed that the hardness value is maximum of 145.80 was achieved. Similarly, maximum tensile strength of 399.76 N/mm^2 was also achieved as seen in Table 2.

Figure 3. Layout of experimental setup & welded work piece

Table 2. Chemical composition of AA2024 material

Element	Cu	Mg	Si	Fe	Cr	Mn	Zn	Ti	Al
wt. %	3.7	1.22	0.5	0.51	0.15	0.32	0.03	0.05	balance

4. OPTIMIZATION OF RESULTS

4.1 Response surface Methodology

Based on the results from Table 3, the following response surface analysis was carried out to understand the effect of friction stir welding process parameters on the joints developed [16-21]. Tables 4 and 5 reveal the influence of process parameters over the results hardness and tensile strength. The models developed were having an R-sq. value of 0.989 and 0.990 for hardness and tensile strength respectively. Based on the P-value of Table 3, all the process parameters taken into consideration have influence on hardness. In a similar manner, all parameters have provided significant influence on tensile strength. Interaction between the process parameters also has the influence over both responses. The response surfaces were plotted to understand effect of interaction among the parameters on welded joints. Figure 4 shows, the combinational effect of parameters on hardness and the same for tensile strength is provided in Figure 5. Improving the rotation speed and traverse speed independently tends to downfall the hardness value. From the contour plots of Figure 4, higher value of hardness is achieved under the combination of 500 rpm rotational and 30 mm/min traverse speeds respectively at all axial loads. Considering tensile strength, the effect of traverse speed is very low compared to other two parameters. The rotational speed initially shows a declining trend of tensile strength up to 750 rpm and improves when the operating condition moves beyond that threshold value. The contour plot of Figure 5 clearly evidences the improvement in tensile strength upon increase in rotational speed higher than 750 rpm with a gradual increase of traverse speed and axial load. Considering traverse speed and axial load combinational effect, tensile strength is maximum whenever both the parameter values are higher.

Table 3. Mechanical property results

Sl. No.	A: Rotational speed (rpm)	B: Traverse speed (mm/min)	C: Axial load (kN)	Weld Hardness	Tensile strength (N/mm^2)
1	800	50	2	137.26	104.33
2	1000	40	6	128.73	272.77
3	800	50	4	134.80	109.52
4	600	60	6	130.60	208.14
5	800	50	4	134.80	109.52
6	800	50	4	134.80	109.52
7	800	50	4	134.80	109.52
8	800	50	6	135.40	164.83
9	600	40	2	136.09	215.00
10	1000	50	4	136.10	268.67
11	800	60	4	134.10	157.23
12	800	30	4	137.36	99.34
13	1000	60	6	132.84	399.76
14	1000	40	2	134.90	207.53
15	600	40	6	145.40	101.49
16	600	60	2	129.05	160.50
17	1000	60	2	145.80	172.91
18	800	50	4	134.80	109.52
19	500	50	4	134.90	265.43
20	800	50	4	134.80	109.52

Table 4. Analysis of variance for hardness

Source	Sum of Squares	df	Mean Square	F Value	p-value Prob > F
Model	330.691	6	55.1151438	161.946657	< 0.0001
A-Rotational speed	0.57056	1	0.57056082	1.67649781	0.2179
B-Transverse speed	11.2637	1	11.26367392	33.0964271	< 0.0001
C-Axial load	10.2779	1	10.2779044	30.1999078	0.0001
AB	169.74	1	169.7403125	498.753597	< 0.0001
AC	112.365	1	112.3650405	330.16593	< 0.0001
BC	26.4628	1	26.4628125	77.7565608	< 0.0001

Table 5. Analysis of variance table for Tensile strength

Source	Sum of Squares	df	Mean Square	F Value	p-value Prob > F
Model	121973.396	9	13552.6	113.5861	< 0.0001
A-Rotational speed	22433.4274	1	22433.43	188.0174	< 0.0001
B-Transverse speed	3917.70493	1	3917.705	32.83479	0.0002
C-Axial load	8220.57779	1	8220.578	68.89771	< 0.0001
AB	202.180913	1	202.1809	1.694504	0.2222
AC	16017.8599	1	16017.86	134.2477	< 0.0001
BC	13021.4698	1	13021.47	109.1346	< 0.0001
A^2	54923.6656	1	54923.67	460.3223	< 0.0001
B^2	322.799829	1	322.7998	2.705427	0.1310
C^2	114.341847	1	114.3418	0.958314	0.3507

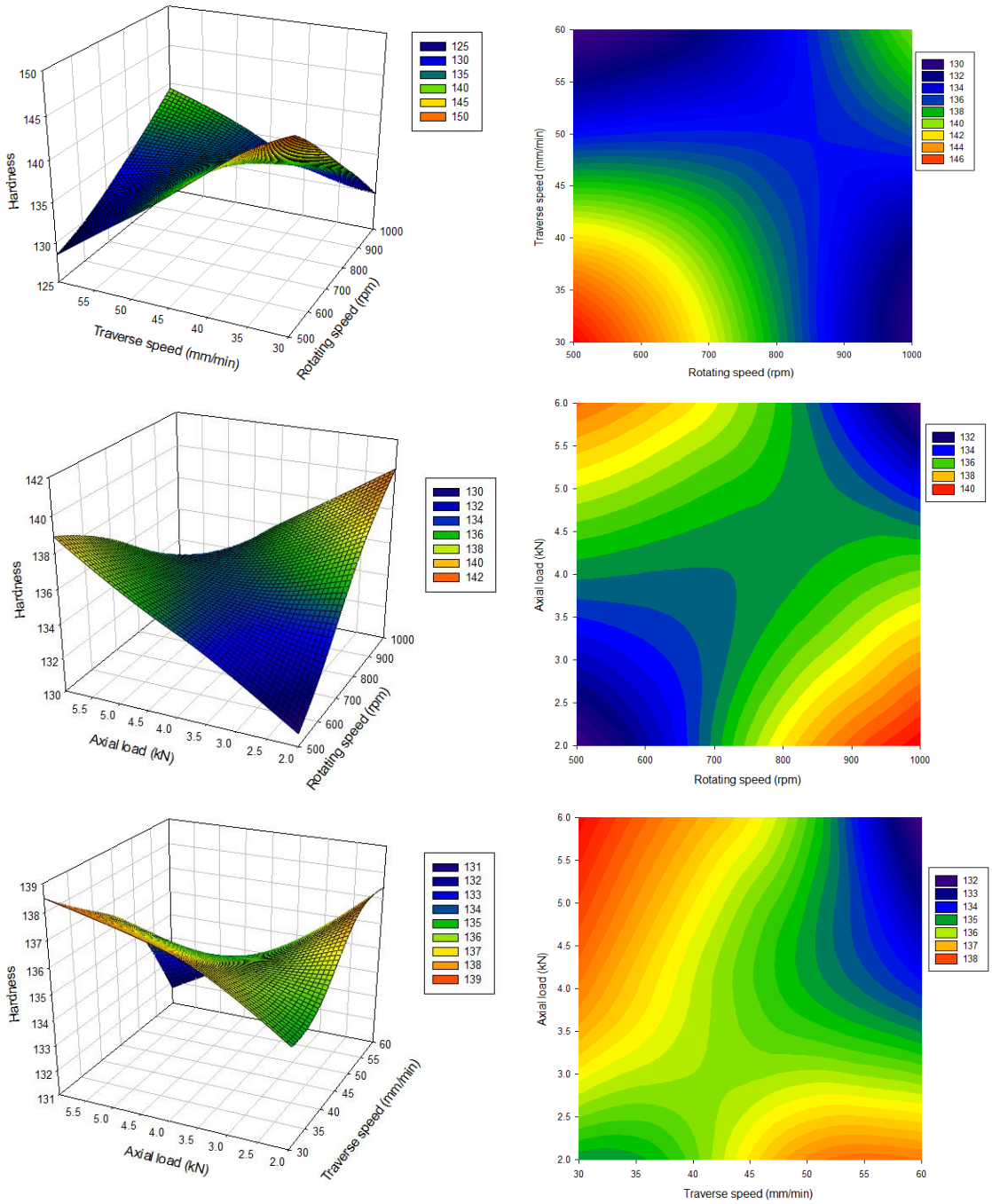

Figure 4. Response surface graphs & contour surface for hardness results

4.2 Analysis of variance

The perturbation plots for experimental results are obtained along with response surface plots for understanding the main effects of parameters. From Figure 6, it is clear that the process parameters have curvature effect on tensile strength and inclined linear effect on weld hardness. Since there is large change in output value for respective changes in input, the sensitivity is very high towards the weld characteristics. Based on the statistical analysis, the regression models were developed for predicting hardness and tensile strength responses with an R-square value of 0.989 and 0.990 respectively. The comparison of experimental value and predicted value is shown in Figure 7. The prediction equations are represented in Equations 1 and 2.

$$\begin{aligned} Hardness = {} & 185.0708 - 0.076552 \times A - 1.57201 \times B \\ & + 11.53547 \times C + 0.00230313 \times A \times B \\ & - 0.00936937 \times A \times C - 0.090937 \times B \times C \end{aligned} \quad (1)$$

$$\begin{aligned} Tensile strength = {} & 2295.25072 - 4.11886 \times A \\ & - 13.14447 \times B - 186.65827 \times C + 0.00251359 \times A \times B \\ & + 0.11187 \times A \times C + 2.01723 \times B \times C + 0.00236067 \times A^2 \\ & + 0.050189 \times B^2 + 1.33 \times C^2 \end{aligned} \quad (2)$$

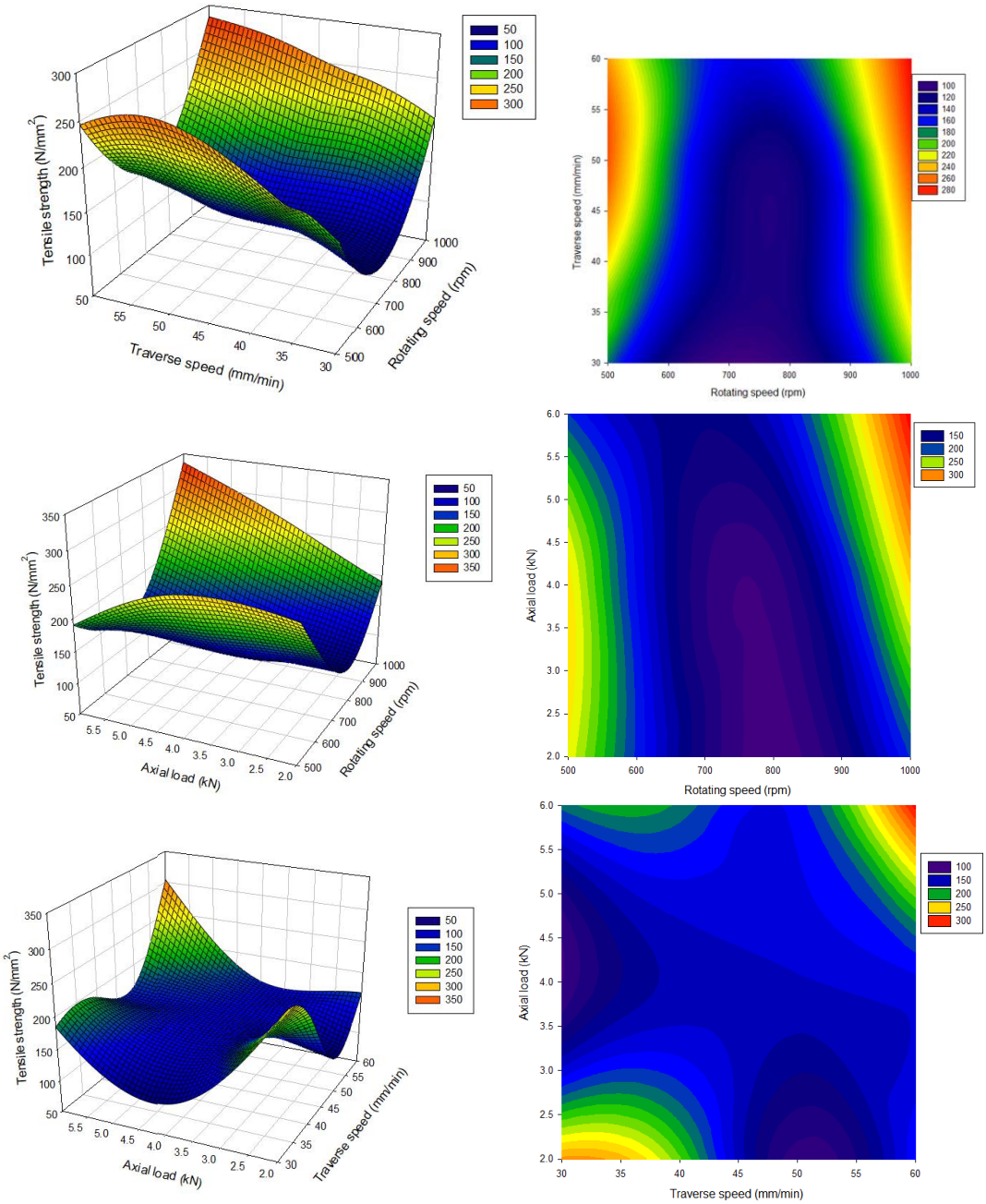

Figure 5. Response surface graphs & contour surface for tensile strength results

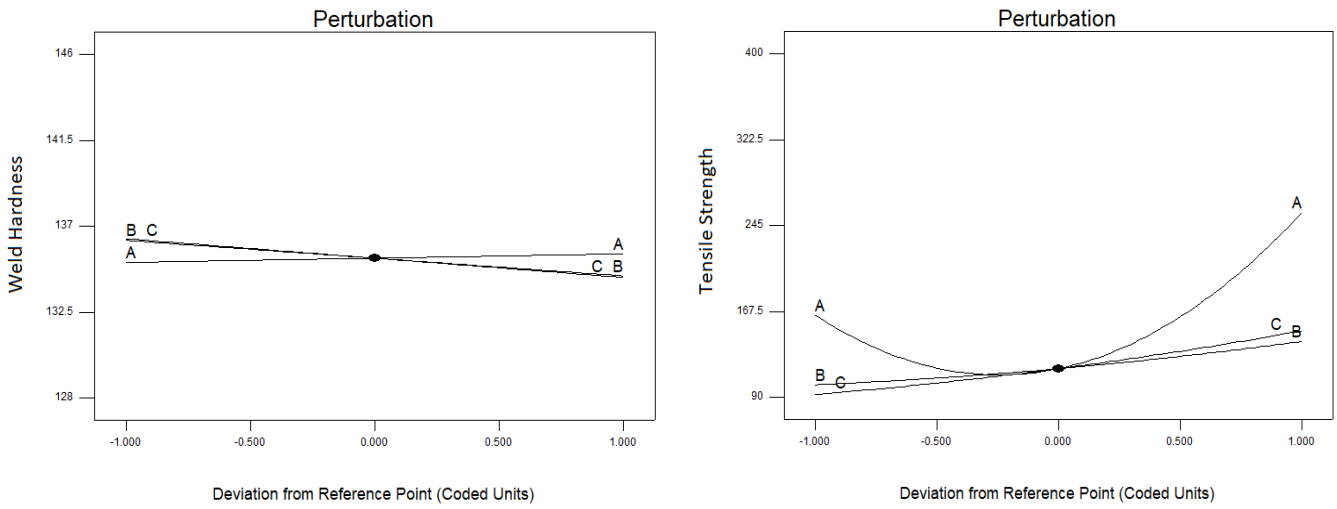

(a) (b)

Figure 6. Perturbation plot for (a) hardness (b) tensile strength

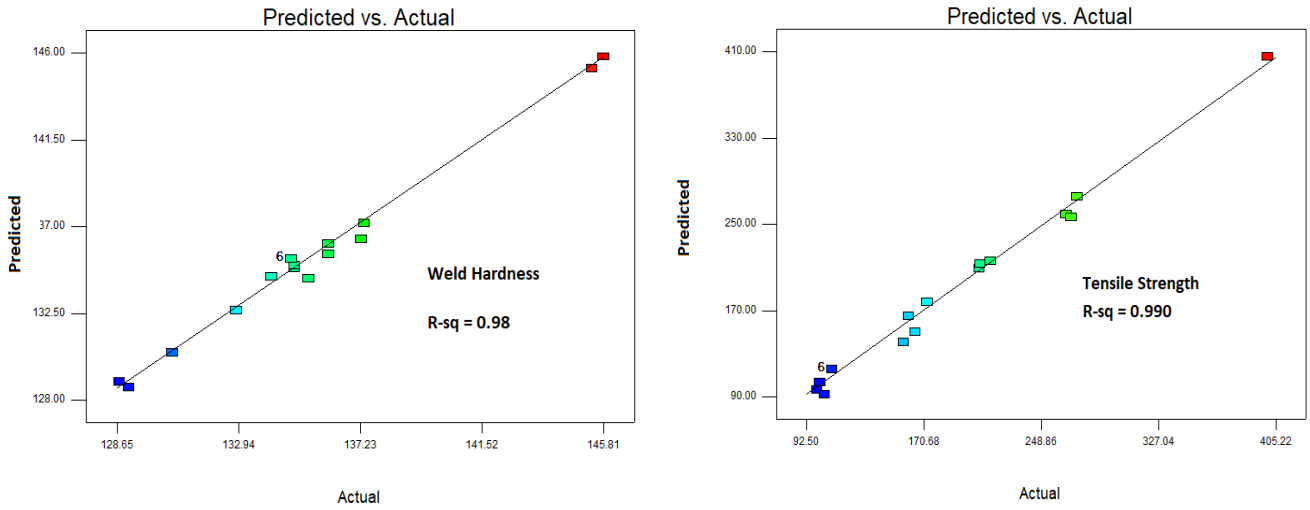

(a) (b)

Figure 7. Experimental vs. predicted plot for (a) hardness (b) tensile strength

4.3 Optimized results and validation

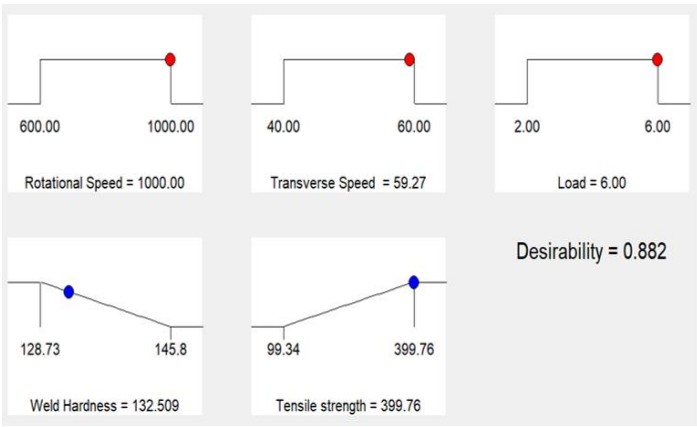

Figure 8. Optimized process parameters for results

The optimization was carried out involving multi-criterion optimization. The objectives of process was set to be maximization for hardness and tensile strength. Equal weightage was assigned to both the responses and a single objective function was framed. Based on that objective function, the optimized results were obtained as per desirability approach. In this work, the optimized results 399.76N/mm^2 for tensile strength and 132.509 for hardness have been achieved with operating parameters of 1000 rpm rotational speed, 59.27 mm/min transverse speed and 6kN load (as shown in Figure 8).

The validation of optimized results so obtained was carried out and results were plotted in Table 5. Since the exact value of transverse speed cannot be set up to decimal precision in machine tools, it was taken as 60 mm/min. Based on the results observed from the Table 6, it is clear that the model is well within the agreeable limit for investigation. The errors were also within 2%.

Table 6. Validation of optimized parameters

	Rotational speed (rpm)	Transverse speed (mm/min)	Axial load (kN)	Weld Hardness	Tensile strength (N/mm^2)
Theoretical	1000	59.27	6	132.509	399.76
Experimented	1000	60	6	132.65	405.24
Percentage of Error				0.10%	1.35%

5. MICROSTRUCTURAL ANALYSIS

The microstructure of components welded by friction stir welding process on 7075-O alloy have been studied [22]. Different parameters were studied during the process like weld speed, traverse speed, number of passes, load applied, etc. The structure was studied by metallurgical tests like optical microscopy and SEM [23-24]. Experimentation were carried to understand about the influence of welding speed on various structural aspects of AA6082. The materials were welded in TIG and MIG followed by ageing treatment. At lower speed of welding, heat developed per unit length was observed to be more and improved fatigue performance of welded joint. At the low and high welding speeds a full and partial softening was predicted. Following the similar approach, microstructural studies were conducted on the present work.

5.1 Morphological Analysis

From the microstructures (shown in Figure 9) it was observed that, the Heat Affected Zone and weld zone areas were more due to higher thermal conductivity of the Al material [25]. Interface welded shown below has differentiated the grains of weld from other zones. The grains of welded zone undergone recrystallization. The grain refinements was due to the double effects of severe plastic deformations and higher operated temperatures. The black dots in the parent material was silicon which is confirmed by EDS analysis shown in Figure 10. Due to Si in Mg (shows circular morphology), the material has high strengthening phases formed during casting [26]. The nugget zone has highly refined and uni-axed grains which will increases the tensile properties of the welded material further. Further the nugget zone has also undergone

severe plastic deformations in Figure 9 and Figure 11. The HAZ has similar elongated grain structure of the base material (BM) since both were recrystallized, parallel to rolled direction and elongated structure. The BM was initially cold rolled before welding which makes the BM to increase in grain size and dispersions of distributed particles.

It can observe that, the grain refinements was decreased in the range of WC> WT> HAZ> Parent material (Shown in Figure 11). The hardness of the samples shown higher values due to the formation of precipitates of Al_2CuMg (known as S phase) at higher heat generated from the friction stir welding. Irregularly shaped Al-Cu-Fe-Mn particles were distributed during welding were observed in HAZ. These precipitates were coarser and their distribution was homogeneous. The dislocations observed in the weld interface (Interface 2 in Figure 11) was due to the formation of Al-Cu-Mg as they have eutectic at 520°C [27]. This particular phase was not seen more in the SEM images which the reason that, the specimen 1 has lower hardness with increased tensile strength. The smaller particles in the welded region was due to higher rotational speed of the tool which redistributed in the matrix.

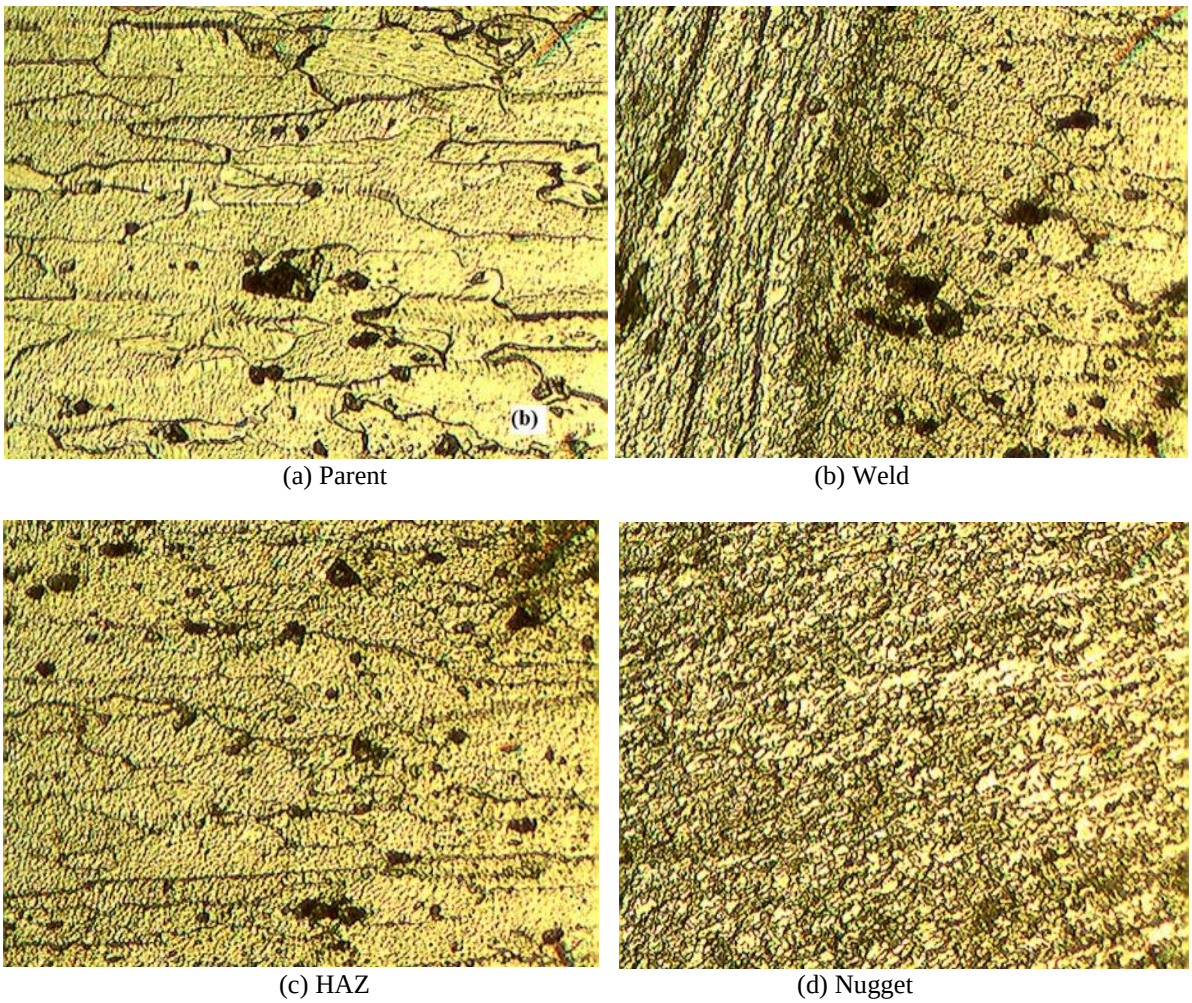

(a) Parent (b) Weld

(c) HAZ (d) Nugget

Figure 9. Optical microscopic image of the welded specimen

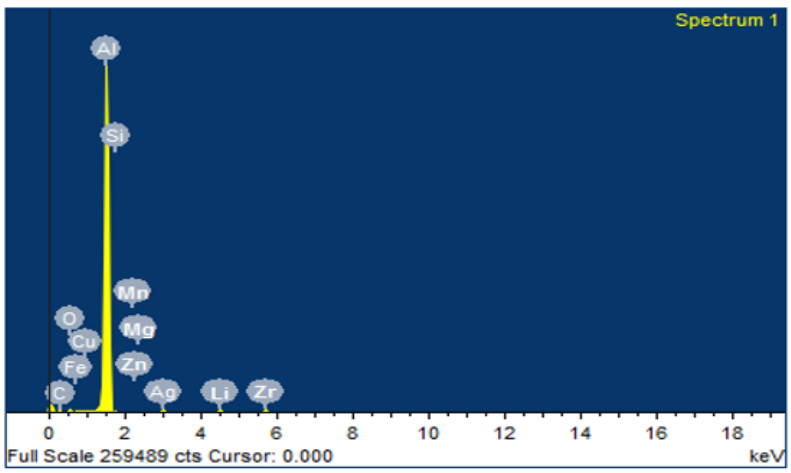

Element	Weight%
C K	0.01
O K	6.94
Al K	87.5
Si K	0.44
Fe K	0.43
Cu K	2.87
Ag L	0.21
Zn K	0.61
Zr K	0.09
Mn K	0.42
Mg K	0.48
Totals	100

Figure 10. EDX result of welded joint

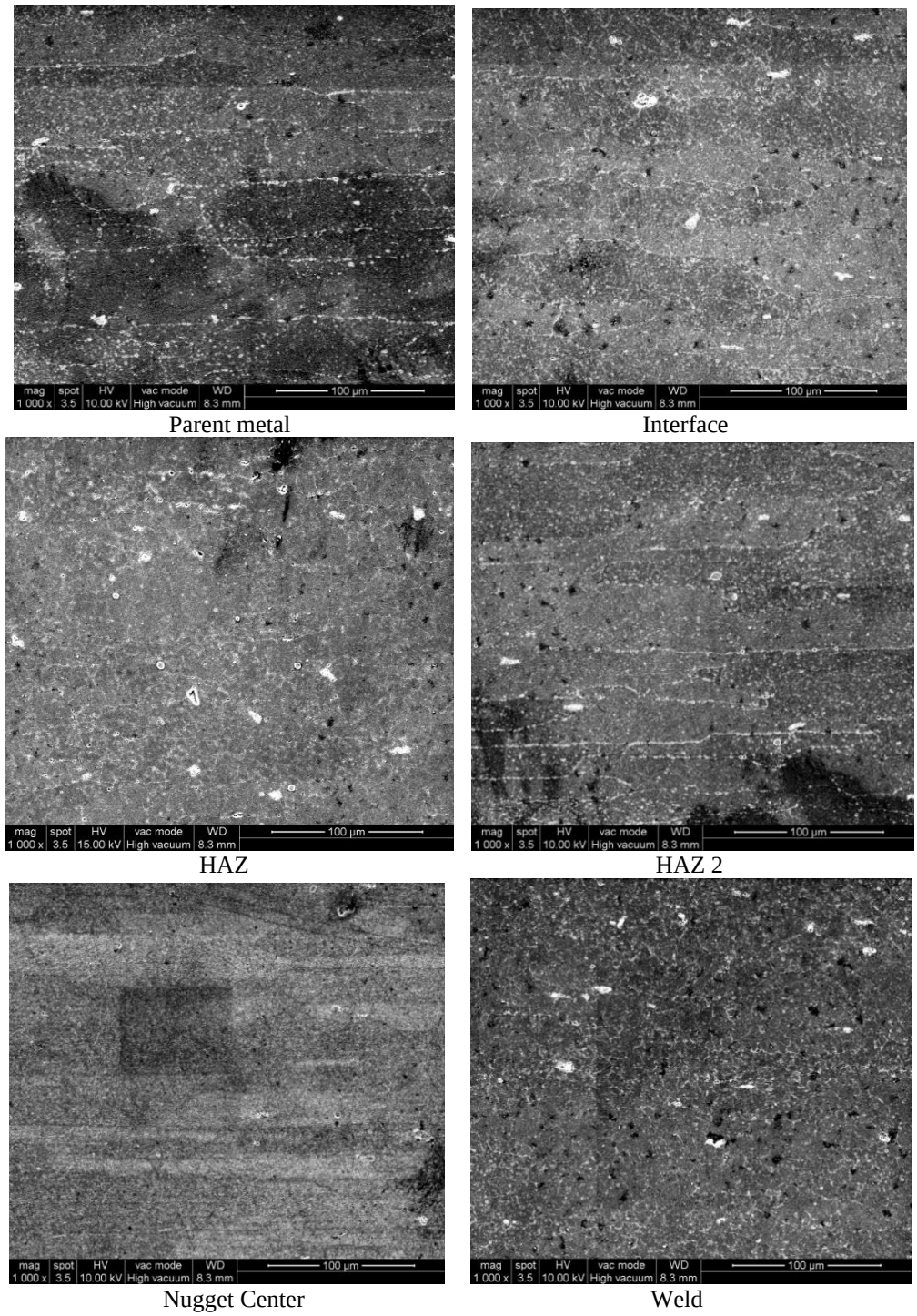

Figure 11. Scanning electron microscope of dissimilar welded joint

5.2 Macrostructure at FSW Joints

Figure 12. Macro structure of the welded joint

From the macro structure we can able to see the tunnel defects (shown in Figure 12). The defects was lower in the 1st specimen which has higher tensile strength. The acceptable hardness were observed in this region due to the reduced softening effect at the boundary of the weld zone. The width of the stir zone was larger and the nugget zone was contracts towards the vortex region. This is due to the reduced heat input during friction welding. We observe that material which is close to the tool experineces intense shear, deformation (compressive) and heat which paves the way for severe plastic deformation, dynamic recrystallization and increases width of weld stir zone.

6. CONCLUSION

Welding of metals with reduced internal stress has been an interest for the decade. The friction stir welding process has

proven to be an effective process for welding softer aluminium material. The various conditions of input parameters were chosen for conducting experiments and results were noted. Based on the results obtained, the weld has higher value of 145.8 hardness and 399.76 N/mm^2 tensile strength with refined grain structure. Regression models were developed for predicting hardness and tensile strength responses with an R-square value of 0.989 and 0.990 respectively. The models were validated with a deviation in value of only 2%. The analysis of microstructure revealed very fine grains at the nugget zone than parent metal. The SEM analysis revealed that the grain refinements was decreased in the range of WC> WT> HAZ> Parent material. Grain refinements were carried out by the double effects of severe plastic deformation at elevated temperatures.

REFERENCES

[1] Moghadam, D.G., Farhangdoost, K., Nejad, R.M. (2016). Microstructure and residual stress distributions under the influence of welding speed in friction stir welded 2024 aluminum alloy. Metallurgical and Materials Transactions B, 47(3): 2048-2062. https://doi.org/10.1007/s11663-016-0611-3

[2] Udayakumar, T., Raja, K., Husain, T.A., Sathiya, P. (2014). Prediction and optimization of friction welding parameters for super duplex stainless steel (UNS S32760) joints. Materials & Design, 53: 226-235. https://doi.org/10.1016/j.matdes.2013.07.002

[3] Genevois, C., Deschamps, A., Vacher, P. (2006). Comparative study on local and global mechanical properties of 2024 T351, 2024 T6 and 5251 O friction stir welds. Materials Science and Engineering: A, 415(1-2): 162-170. https://doi.org/10.1016/j.msea.2005.09.032

[4] Fu, R.D., Zhang, J.F., Li, Y.J., Kang, J., Liu, H.J., Zhang, F.C. (2013). Effect of welding heat input and post-welding natural aging on hardness of stir zone for friction stir-welded 2024-T3 aluminum alloy thin-sheet. Materials Science and Engineering: A, 559: 319-324. https://doi.org/10.1016/j.msea.2012.08.105

[5] Genevois, C., Fabregue, D., Deschamps, A., Poole, W.J. (2006). On the coupling between precipitation and plastic deformation in relation with friction stir welding of AA2024 T3 aluminium alloy. Materials Science and Engineering: A, 441(1-2): 39-48. https://doi.org/10.1016/j.msea.2006.07.151

[6] Moradi, M.M., Aval, H.J., Jamaati, R., Amirkhanlou, S., Ji, S. (2018). Microstructure and texture evolution of friction stir welded dissimilar aluminum alloys: AA2024 and AA6061. Journal of Manufacturing Processes, 32: 1-10. https://doi.org/10.1016/j.jmapro.2018.01.016

[7] Safarbali, B., Shamanian, M., Eslami, A. (2018). Effect of post-weld heat treatment on joint properties of dissimilar friction stir welded 2024-T4 and 7075-T6 aluminum alloys. Transactions of Nonferrous Metals Society of China, 28(7): 1287-1297. https://doi.org/10.1016/S1003-6326(18)64766-1

[8] Rafiei, R., Shamanian, M., Fathi, M.H., Khodabakhshi, F. (2018). Dissimilar friction-stir lap-welding of aluminum-magnesium (AA5052) and aluminum-copper (AA2024) alloys: microstructural evolution and mechanical properties. The International Journal of Advanced Manufacturing Technology, 94(9-12): 3713-3730. 10.1007/s00170-017-0964-z

[9] Chanakyan, C., Sivasankar, S., Meignanamoorthy, M., Ravichandran, M., Muralidharan, T. (2020). Experimental investigation on influence of process parameter on friction stir processing of AA6082 using response surface methodology. Materials Today: Proceedings, 21: 231-236. https://doi.org/10.1016/j.matpr.2019.05.384

[10] Li, J., Su, M., Qi, W., Wang, C., Zhao, P., Ni, F., Liu, K. (2020). Mechanical property and characterization of 7A04-T6 aluminum alloys bonded by friction stir welding. Journal of Manufacturing Processes, 52: 263-269. https://doi.org/10.1016/j.jmapro.2020.02.018

[11] Mehta, K.P., Carlone, P., Astarita, A., Scherillo, F., Rubino, F., Vora, P. (2019). Conventional and cooling assisted friction stir welding of AA6061 and AZ31B alloys. Materials Science and Engineering: A, 759: 252-261. https://doi.org/10.1016/j.msea.2019.04.120

[12] Choi, J.W., Liu, H., Fujii, H. (2018). Dissimilar friction stir welding of pure Ti and pure Al. Materials Science and Engineering: A, 730: 168-176. https://doi.org/10.1016/j.msea.2018.05.117

[13] Shen, Z., Ding, Y., Gopkalo, O., Diak, B., Gerlich, A.P. (2018). Effects of tool design on the microstructure and mechanical properties of refill friction stir spot welding of dissimilar Al alloys. Journal of Materials Processing Technology, 252: 751-759. https://doi.org/10.1016/j.jmatprotec.2017.10.034

[14] Kumar, R., Singh, R., Ahuja, I.P.S., Penna, R., Feo, L. (2018). Weldability of thermoplastic materials for friction stir welding-A state of art review and future applications. Composites Part B: Engineering, 137: 1-15. https://doi.org/10.1016/j.compositesb.2017.10.039

[15] Shanavas, S., Dhas, J.E.R. (2017). Parametric optimization of friction stir welding parameters of marine grade aluminium alloy using response surface methodology. Transactions of Nonferrous Metals Society of China, 27(11): 2334-2344. https://doi.org/10.1016/S1003-6326(17)60259-0

[16] Dinesh, S., Karthikeyan, T., Vijayan, V. (2020). Powder mixed electrical discharge machining of oil hardened non shrinking steel die steel–Optimization and investigation. Materials Today: Proceedings. https://doi.org/10.1016/j.matpr.2020.04.909

[17] Dinesh, S., Antony, A.G., Rajaguru, K., Vijayan, V. (2016). Investigation and prediction of material removal rate and surface roughness in CNC turning of EN24 alloy steel. Asian Journal of Research in Social Sciences and Humanities, 6(8): 849-863.

[18] Dinesh, S., Antony, A.G., Karuppusamy, S., Kumar, B. S., Vijayan, V. (2016). Experimental investigation and optimization of machining parameters in CNC turning operation of duplex stainless steel. Asian Journal of Research in Social Sciences and Humanities, 6(10): 179-195. 10.5958/2249-7315.2016.01006.6

[19] Dinesh, S., Antony, A.G., Rajaguru, K., Parameswaran, P. (2018). Comprehensive analysis of wire electric discharge machining process in machining high chromium high carbon steel. International Journal of Mechanical and Production Engineering Research and Development (IJMPERD), 8(1): 65-74.

[20] Dinesh, S., Prabhakaran, M., Antony, A.G., Rajaguru, K., Vijayan, V. (2017). Investigation and optimization of

machining parameters in processing AISI 4340 alloy steel with electric discharge machining. Int. J. Pure and Applied Mathematics, 117(16): 385-391.

[21] Hynes, N.R.J., Velu, P.S. (2018). Effect of rotational speed on Ti-6Al-4V-AA 6061 friction welded joints. Journal of manufacturing processes, 32: 288-297. https://doi.org/10.1016/j.matpr.2020.06.343

[22] Girish, G., Anandakrishnan, V. (2019). Investigations on microstructural and texture evolution during recursive friction stir processing of aluminium 7075 alloy. Materials Research Express, 6(12): 126574. https://doi.org/10.1088/2053-1591/ab58ed

[23] Ericsson, M., Sandström, R. (2003). Influence of welding speed on the fatigue of friction stir welds, and comparison with MIG and TIG. International Journal of Fatigue, 25(12): 1379-1387. https://doi.org/10.1016/S0142-1123(03)00059-8

[24] Udayakumar, T., Raja, K., Abhijit, A.T., Sathiya, P. (2013). Experimental investigation on mechanical and metallurgical properties of super duplex stainless steel joints using friction welding process. Journal of Manufacturing Processes, 15(4): 558-571. https://doi.org/10.1016/j.jmapro.2013.06.010

[25] Hynes, N.R.J., Velu, P.S. (2018). Effect of rotational speed on Ti-6Al-4V-AA 6061 friction welded joints. Journal of manufacturing processes, 32: 288-297. https://doi.org/10.1016/j.jmapro.2018.02.014

[26] Gupta, A.K., Lloyd, D.J., Court, S.A. (2001). Precipitation hardening in Al–Mg–Si alloys with and without excess Si. Materials Science and Engineering: A, 316(1-2): 11-17. https://doi.org/10. 1016/S0921-5093(01)01247-3.

[27] Bauri, R., Yadav, D., Suhas, G. (2011). Effect of friction stir processing (FSP) on microstructure and properties of Al–TiC in situ composite. Materials Science and Engineering: A, 528(13-14): 4732-4739.https://doi.org/10.1016/j.msea.2011.02.085